Computer calculations of the MgO-SiO2-AlO1.5 ternary and higher order phase diagrams through thermodynamic analysis of phase equilibria

by Matthew James Scanlon

A thesis submitted in partial fulfillment of the requirements for the degree of Doctor of Philosophy in Chemistry

Montana State University

Abstract:
Published data on the MgO-Sio2-A101.5 ternary system, along with the binaries and single component phases, are analysed in order to develop a computer model for the ternary system. In doing this a very useful relationship between the bulk modulus and coefficient of thermal expansion using the Murnaghan logarithmic equation of state is derived, thus allowing dK/dT to be calculated from thermal expansion measurements. Also, the alpha-beta transition in quartz was analysed using Pippard's theory of second order phase transitions, accurate X-ray data and the pressure dependence of the transition temperature.

Full equations of state for quartz are given up to 1900 K and 4000 MPa. The phase diagram is also calculated.

From analysis of the phase equilibria in the MgO-SiO2 system and the enthalpy of vitrification of MgSi03, the enthalpies of fusion of enstatite and forsterite were refined. The final best values for the heats of fusion were 48.8 ± 4 kJ/mole and 92.9 ± 12 kJ/mole respectively.

Also phase diagrams are calculated at 0.1 and 1000 MPa using Redlich-Kister coefficients.

Methods of dealing with three, four, and five component systems are developed using Redlich-Kister equations. Portions of the phase diagrams for the MgO-SiO2 A101.5 ternary and the FeO-Feo1.5-Cao-Sio1.5 system are calculated.

COMPUTER CALCULATIONS OF THE MgO-SiO_2-$AlO_{1.5}$ TERNARY AND HIGHER ORDER PHASE DIAGRAMS THROUGH THERMODYNAMIC ANALYSIS OF PHASE EQUILIBRIA

by

Matthew James Scanlon

A thesis submitted in partial fulfillment
of the requirements for the degree

of

Doctor of Philosophy

in

Chemistry

MONTANA STATE UNIVERSITY
Bozeman, Montana

March 1988

APPROVAL

of a thesis submitted by

Matthew James Scanlon

This thesis has been read by each member of the thesis committee and has been found to be satisfactory regarding content, English usage, format, citations, bibliographic style, and consistency, and is ready for submission to the College of Graduate Studies.

3/21/88
Date

Reed Howald
Chairperson, Graduate Committee

Approved for the Major Department

3/13/88
Date

Bradford Philip Mundy
Head, Major Department

Approved for the College of Graduate Studies

3-22-88
Date

Michael Malone
Graduate Dean

STATEMENT OF PERMISSION TO USE

In presenting this thesis in partial fulfillment of the requirements for a doctoral degree at Montana State University, I agree that the Library shall make it available to borrowers under rules of the Library. I further agree that copying of this thesis is allowable only for scholarly purposes, consistent with "fair use" as prescribed in the U. S. Copyright Law. Requests for extensive copying or reproduction of this thesis should be referred to University Microfilms International, 300 North Zeeb Road, Ann Arbor, Michigan 48106, to whom I have granted "the exclusive right to reproduce and distribute copies of the dissertation in and from microfilm and the right to reproduce and distribute by abstract in any format."

Signature Matthew J. Sommer

Date 3/16/88

ACKNOWLEDGMENT

My gratitude and thanks to all the people who helped and supported me through thick and thin during the course of this work. Reed Howald gave a tremendous amount of support and encouragement during the work and the writing, and Elaine Howald helped in the proof reading. A special thank you to Pat and Gayle Callis for their support and their friendship.

TABLE OF CONTENTS

INTRODUCTION. 1

The Redlich-Kister Equations 3

The Two Component Phase Diagram. 7

Extended Redlich-Kister Notation 9

The Higher Component Systems 12

THE ONE COMPONENT PHASES. 14

Equations of State for Magnesium Oxide 14

Equations of State for Silicon Dioxide 28
The Alpha Quartz to Beta Quartz Transition. . 30
The Equation of State for Beta Quartz 42
Equation of State of Alpha Quartz 49
Equation of State for Coesite 52
The Equation of state for Cristobalite. . . . 60
Equation of State for Silicon Dioxide Liquid. 66

Equations of State for Aluminum Oxide. 68
Aluminum Oxide (C, Corundum). 69
Aluminium Oxide (Liquid). 74

The Stochiometric Phases 75
Forsterite. 75
Enstatite (Magnesium Silicate). 76
Spinel (Magnesium Aluminate). 77
Cordierite. 83

THE BINARY SYSTEMS. 86

The Magnesia-Silica Binary 86
The Enthalpy of Fusion of Magnesium Oxide . . 93
The Entropy of Mixing 95
The Heat Capacity 98
The Phase Diagram 102

The Alumina-Silica Binary. 102

THE TERNARY SYSTEM MAGNESIUM OXIDE-SILICA-ALUMINA . . .112

THE FeO-$FeO_{1.5}$-SiO_2-$AlO_{1.5}$-CaO SYSTEM. 124

The FeO-$FeO_{1.5}$ System. 124

SUMMARY 136

REFERENCES CITED. 138

LIST OF TABLES

Table		Page
1.	The Redlich-Kister coefficients for a three component system, through seventh power in mole fraction.	10
2.	Redlich-Kister coefficients and their subscripts correlated with their corresponding powers.	12
3.	The three and four component Redlich-Kister coefficients.	13
4.	Calculated molar volumes for MgO.	22
5.	The equations of state, heat capacity equations and selected thermodynamic properties of MgO (c) and MgO (l)	23
6.	Values reported for the enthalpy change between alpha quartz at 298.15 k and beta quartz at 1000 K.	29
7.	Calculated equilibrium constants at various temperatures between our's and Robie et al's. equation of state for Beta quartz	29
8.	The function $F(\theta)$ representing the difference in volume of alpha quartz from a fully disordered beta quartz at the same temperature.	39
9.	The entropy and enthalpy changes for alpha quartz near the lambda point	41
10.	The equations of state, heat capacity equations and selected thermodynamic properties of alpha and beta quartz.	46
11.	Comparison of the thermodynamic values for beta quartz and coesite at high pressures and temperatures.	50

Table Page

12. Comparison of the polynomial fit and Pippard calculations for the thermodynamic propreties of alpha and beta quartz 60 K below the lamda transition. 55

13. The equation of state, heat capacity equations and selected thermodynamic properties of coesite and high coesite. 56

14. The thermodynamic properties of cristobalite. . . . 61

15. The equations of state, heat capacity equations and selected thermodynamic properties of cristobalite and liquid quartz. 65

16. The equations of state, heat capacity equations and selected thermodynamic properties of aluminum oxide, corundum and liquid. 70

17. The equation of state, heat capacity equation and selected thermodynamic properties of forsterite (Mg_2SiO_4). 76

18. The equations of state, heat capacity equations and selected thermodynamic properties of the three forms of $MgSiO_3$; enstatite, protoenstatite and orthoenstatite. 78

19. The equation of state, heat capacity equation and selected thermodynamic properties of spinel ($MgAl_2O_4$) 80

20. ΔS and ΔV of disproportionation for $MgAl_2O_4$ 85

21. The equation of state, heat capacity equation and selected thermodynamic properties of cordierite ($Mg_2Al_4SiO_{18}$) 85

22. Published estimates of the enthalpy of fusion of various compounds in the MgO-SiO_2 system. 87

23. Excess enthalpies of mixing of MgO and SiO_2 for various models at a mole fraction of 0.5. 88

Table Page

24. Calculated equilibrium constants for the reaction: $2Mg_2SiO_4$ (l) = $Mg_3Si_2O_7$ + MgO(l) at x MgO^2 = 0.7, where z is the number of moles of $Mg_3Si_2O_7$. 95

25. Redlich-Kister coefficients for acidic and basic $MgO-SiO_2$. 107

26. Redlich-Kister coefficients for the $AlO_{1.5}-SiO_2$ solid and liquid systems. 108

27. The matrix MTOOP for calculating ternary Redlich-Kister coefficients 115

28. The transformation matrix, CNN, from the Redlich-Kister vector N^n_{123} to the vector N^n_{312} 116

29. Calculated Redlich-Kister coefficients for excess enthalpy from the Toop-Muggianu interpolation along with our final selected values for the $MgO-SiO_2-AlO_{1.5}$ ternary at 1800 117

30. Calculated excess enthalpies at 1800 K using the Redlich-Kister coefficients from the Toop-Muggiana interpolation and our final selected values for the $MgO-SiO_2-AlO_{1.5}$ ternary 120

31. Redlich-Kister terms through F for the ternary system $AlO_{1.5}-SiO_2-MgO$. 121

32. The heat capacity equations and thermodynamic properties of various stoichiometric compounds in the $FeO-FeO_{1.5}-SiO_2-AlO_{1.5}-CaO$ system 126

33. Redlich-Kister coefficients for the $FeO-FeO_{1.5}$ solid binary. 128

34. Redlich-Kister coefficients for the $FeO-FeO_{1.5}$ liquid binary 129

LIST OF FIGURES

Figure Page

1. The coefficient of thermal expansion of MgO. The S shaped line with alternating long and short dashes represents the values used in ref.25. The straight dashed line is $.0000435+1.0\times10^{-8}(T-1000)$. The solid line shows the values selected in this work. Above 300K the solid line is that calculated from ref.16, 17, and 20. 15

2. The isoentropic bulk modulus for MgO. The solid line is calculated from the theory presented here. The experimental values are from Spetzler, black circles; Soga and Anderson, open circles; and from Anderson and Andreatch, diamonds. 21

3. Contour lines for the Gruniesen parameter, δ, for MgO on a P-T field. The contour interval is 0.01, except that at high temperatures dotted lines at 0.02 intervals are also shown. 25

4. Gruneisen parameters, δ, for MgO plotted versus volume for the three pressures 0.01, 5000, and 10000 MPa. The circles represent calculated values at 300, 400, and 600 K. The dotted line is for $\gamma = 0.12652\ V^{1.0059}$ 26

5. Heat capacity, Cp, for alpha quartz near the lambda temperature. The solid line represents our calculated values. The experimental points of Moser and Sinel'nikov are shown as open and filled circles respectively 32

6. Cell demensions for alpha and beta quartz versus temperature. Our calculated fits to the values of Ackerman and Sorrel (filled circles) are shown as solid lines. Older experimental values of Jay (1939) and Berger et al.(1966) are shown as open circles. 33

Figure Page

7. Volumes of beta quartz at 0.1 MPa and at the lambda point plotted versus temperature. 43

8. Our calculated contour lines for the volume of beta quartz. 47

9. Our calculated contour lines for the entropy of beta quartz 48

10. $(dT/dP)_S = \alpha VT/Cp$ at 800 K. The solid line is our calculated curve. The open circles are the experimental values of Boehler. 53

11. $(dT/dP)_S = \alpha VT/Cp$ at 1000 K. The solid line is our calculated curve. The open circles are the experimental values of Boehler. 54

12. Heat capacity values for coesite (solid line) and cristobalite (dashed lines) 57

13. Calculated phase diagram for SiO_2. Filled circles are from Boehler (1982), Bohen and Boetcher (1982), Mirwald and Massone (1980), with the values of Boyd and England, (1960), as open circles. 59

14. The thermal expansion coefficient of aluminum oxide versus temperature. 72

15. The adiabatic bulk modulus of $AlO1.5$ versus temperature. The filled circles are values from Tefft (1966); the open circles are our calculated values and the solid diamonds are the values of Soga and Anderson(1967) 73

16. The calculated phase diagram for $MgSiO_3$. The experimental points shown are those of Grover (1972) and Boyd and England (1965). 79

17. Contour lines for the volume of $MgAl_2O_4$, Spinel, as a function of temperature as reported by Howald, et al 81

18. Countour lines showing ΔV for the reaction $MgAl_2O_4(c) = MgO(c) + 2AlO_{1.5}(c)$. 82

Figure Page

19. Equilibrium line for the spinel disproportionation as calculated in this work. 84

20. Various calculated excess enthalpies for the $MgO-SiO_2$ phase diagram. 89

21. Corrected Gibbs free energy (G -382.14T) versus mole fraction of SiO_2 for the system $MgO-SiO_2$ . . . 91

22. Entropy of mixing versus the mole fraction of SiO_2 in the system $MgO-SiO_2$. Circles, open squares and filled squares are from Lin and Pelton, ideal mixing and this work respectively 99

23. Excess heat capacity versus mole fraction of SiO_2 at 2123 K for the $MgO-SiO_2$ system 101

24. The calculated phase diagram at 0.1 MPa for the $MgO-SiO_2$ system 103

25. Activities of SiO_2. Open circles are calculated from our Redlich-Kister coefficients, filled diamonds are from S. Kambayashi and E. Kato 104

26. Activities of MgO. Filled diamonds are calculated from our Redlich-Kister coefficients, open circles are from S. Kambayashi and E. Kato. 105

27. The Calculated phase diagram at 1000 MPa. for the $MgO-SiO_2$ system 106

28. The calculated contour lines for the $MgO-SiO_2-AlO_{1.5}$ ternary system. 122

29. The calculated phase fields for the ternary system $MgO-SiO_2-AlO_{1.5}$ 123

30. Contour lines in the $AlO_{1.5}-SiO_2-FeO_x$ system versus weight fraction calculated as $FeO_{1.5}$ for H_2O/H_2 = 1.3. Temperatures are given in 200 degree Fahrenheit intervals 131

31. Contour lines in the $AlO_{1.5}-SiO_2-FeO_x$ system at 5% CaO by weight and H_2O/H_2 = 1.3. 132

32. Contour lines in the $AlO_{1.5}-SiO_2-FeO_x$ system at 10% CaO by weight and H_2O/H_2 = 1.3 133

Figure Page

33. Contour lines in the $AlO_{1.5}$-SiO_2-FeO_x system at 20% CaO by weight and H_2O/H_2 = 1.3 134

34. Contour lines in the $AlO_{1.5}$-SiO_2-FeO_x system at 20% CaO by weight and H_2O/H_2 = 1.3 135

ABSTRACT

Published data on the MgO-SiO_2-$AlO_{1.5}$ ternary system, along with the binaries and single component phases, are analysed in order to develop a computer model for the ternary system. In doing this a very useful relationship between the bulk modulus and coefficient of thermal expansion using the Murnaghan logarithmic equation of state is derived, thus allowing dK/dT to be calculated from thermal expansion measurements. Also, the alpha-beta transition in quartz was analysed using Pippard's theory of second order phase transitions, accurate X-ray data and the pressure dependence of the transition temperature. Full equations of state for quartz are given up to 1900 K and 4000 MPa. The phase diagram is also calculated.

From analysis of the phase equilibria in the MgO-SiO_2 system and the enthalpy of vitrification of $MgSiO_3$, the enthalpies of fusion of enstatite and forsterite were refined. The final best values for the heats of fusion were 48.8 ± 4 kJ/mole and 92.9 ± 12 kJ/mole respectively. Also phase diagrams are calculated at 0.1 and 1000 MPa using Redlich-Kister coefficients.

Methods of dealing with three, four, and five component systems are developed using Redlich-Kister equations. Portions of the phase diagrams for the MgO-SiO_2-$AlO_{1.5}$ ternary and the FeO-$FeO_{1.5}$-CaO-SiO_2-$AlO_{1.5}$ system are calculated.

INTRODUCTION

In order to calculate a multicomponent phase diagram, one must to be able to calculate equilibrium constants for all the reactions between the various phases present. For the MgO-SiO_2-Al_2O_3 ternary system the one component systems are pure MgO, SiO_2 and $AlO_{1.5}$. The additional pure stoichiometric solids Mg_2SiO_4, $MgSiO_3$, $MgAl_2O_4$ and $Al_6Si_2O_{13}$ are also formed in this phase diagram.

In a one component phase diagram, volume, temperature and pressure can be modelled by fitting the volume data to a power series in both temperature and pressure. The computer program we are using can handle up to thirty-five of these terms, so that the calculated volumes are accurate over a wide range of temperatures and pressures. Once the coefficients for these polynomial terms are calculated the volume contour lines for the individual species can be determined. The representation of volume as a function of temperature and pressure is known as the equation of state for a pure material.

The heat capacity, C_P, at constant pressure can be fit to a power series of the form

$$C_P = A + B(T - T_o) + C(T - T_o)^2 + D(T - T_o)^3 + \ldots \quad (1)$$

where A, B, C and D are constants, T is the temperature and T_o is a standard temperature of 1000 K or 298.15 K. The derivative of the heat capacity with respect to pressure is

$$(dC_P/dP)_T = VT(d\ /dT)_p - T\alpha^2V$$
$$= -T(d^2V/dT^2)_P \qquad (2)$$

where α the thermal expansion coefficient is $1/V(dV/dT)_p$. Therefore, the heat capacity can be calculated at various pressures from the volume polynomials described earlier.

The temperature and pressure dependence of the enthalpy of a substance is related to the heat capacity and the volume through the equation

$$dH = (dH/dT)_p dT + (dH/dP)_T dP \qquad (3)$$

which becomes

$$dH = C_p dT + (V - T\alpha V)dP \qquad (4)$$

respectively. Thus, with a value for the enthalpy at a particular temperature and pressure referenced from the heats of formation from the elements at 298.15 K and the volume polynomial one can calculate the enthalpy at any temperature and pressure. We have choosen 1000 K and .1 MPa. as our standard temperature and pressure.

The equilibrium constant is related to the standard Gibbs free energies of the components involved in the equilibria through the equation

$$\Delta G°_T = -RT\ln(K_T). \qquad (5)$$

Since $\Delta G = \Delta H - T\Delta S$, the equilibrium constant can also be expressed by the equation

$$K_T = \exp(-\Delta G°/RT) = \exp(-\Delta H°/RT)\ \exp(\Delta S°/R) \quad (6)$$

or converting to base 10 and using J/mole yields

$$K_T = 10^{(-\Delta H°/19.14464\ T)}\ 10^{(\Delta S°/19.14464)}. \quad (7)$$

However in the literature, free energy is often tabulated in the form of Planck's function, Y. Planck's function includes the temperature dependence of both the enthalpy and the entropy and is defined as

$$Y_T = (G°_T - H°_{298.15})/T. \quad (8)$$

The pressure dependence of Plancks function is determined from the heat capacities pressure dependence. Thus the equation for the equilibrium constant can be written

$$K_T = 10^{(-\Delta H°298.15/19.14464T)}\ 10^{(\Delta Y_T/19.14464)}. \quad (9)$$

With the information described above gathered and incorporated into the computer, the properties of any compound at any temperature and pressure for which the equations are accurate can be calculated.

The Redlich-Kister Equations

In order to describe a two component phase diagram, one must model the thermodynamic properties as a function of mole fraction (x). There are a variety of methods of modelling phase diagrams in terms of chemical equilibria using known equilibrium constants.[1,2,3] Also sublattice

models have been proposed and used sucessfully for spinels.[4,5,6,7] However, it is difficult to do calculations of phase equilibria when various types of equations are being used. Therefore it is an advantage to use power series of a standard form, which are able to fit the most complex systems.

The quantities that have to be modelled in a two component system are the partial molal quantities of both components and the excess quantity. The partial molal quantity and the excess quantity are defined through the following equations

$$\overline{Q}_1 = (dQ/dn_1)_{n_2,T,P} \tag{10}$$

$$Q = n_1Q_1^\circ + n_2Q_2^\circ + (n_1 + n_2)Q^e \tag{11}$$

where $\overline{Q}_1$ is the partial molal quantity of component 1, Q is the thermodynamic quantity, Q° is the thermodynamic quantity of the pure substance, and Q^e is the excess molal quantity. Any power series representation of a two component system must satisfy certain conditions. As the mole fraction of a particular component, X_i, approaches 1 the partial molal quantity, $\overline{Q}_i$, approaches the value of the molal quantity of the pure substance Q°. Also, the excess quantity, Q^e, must approach zero.

The earliest proposed set of power series equations is that proposed by Margules[8] in 1895. The Margules equations are

$$\bar{Q}_1 - Q_1^\circ = (1 - x_1)^2(A_1 + B_1x_1 + C_1x_1^2 + D_1x_1^3 + \ldots)$$

$$\bar{Q}_2 - Q_2^\circ = x_1^2(A_2 + B_2x_1 + C_2x_1^2 + D_2x_1^3 + \ldots) \quad (12)$$

$$Q^e = x_1x_2(A_e + B_ex_1 + C_ex_1^2 + D_ex_1^3 + \ldots).$$

These equations satisfy the above conditions, however, each equation has a different set of coefficients, and the mole fraction terms within an equation are not orthogonal. Two terms are orthoganol if the integral of the product of the terms over all space is zero. If the mole fraction terms are orthogonal, then the four term series would have the same first three coefficients as the coefficients in a three term series.

Bale and Pelton[9,10] have proposed the following set of equations to model the thermodynamic quantities

$$\bar{Q}_1 - Q_1^\circ = (1-x_1)^2 \sum_{i=0}^{n} a_iP_i(x_i)$$

$$\bar{Q}_2 - Q_2^\circ = x_1^2 \sum_{i=0}^{n} b_iP_i(x_i) \quad (13)$$

$$Q^e = x_1x_2 \sum_{i=0}^{n} q_iP_i(x_i)$$

where $P_i(x_i)$ are the standard Legendre polynomials. These polynomials are completely orthogonal; however, they still have different coefficients for the mole fraction terms in each equation.

O. Redlich and A. T. Kister[11,12] in 1948 proposed the following set of power series equations

$$\bar{Q}_1 - Q_1^\circ = x_2^2[A + B(4x_1 - 1) + C(6x_1 - 1)(2x_1 - 1) + D(8x_1 - 1)(2x_1 - 1)^2 + \ldots] \quad (14)$$

$$\bar{Q}_2 - Q_2^\circ = x_1^2[A + B(4x_1 - 1) + C(6x_1 - 5)(2x_1 - 1) + D(8x_1 - 7)(2x_1 - 1)^2 + \ldots] \quad (15)$$

$$Q^e = x_1x_2[A + B(2x_1 - 1) + C(2x_1 - 1)^2 + D(2x_1 - 1)^3 + \ldots]. \quad (16)$$

These equations are not completely orthogonal, however, the same coefficients A, B, and C appear in all three equations.

The reason the coefficients are the same is that the mole fraction terms for $\bar{Q}_1 - Q_1^\circ$ and $\bar{Q}_2 - Q_2^\circ$ are derived from the excess partial molal quantity Q^e. From the definition of the partial molal quantity and the expression for the thermodynamic quantity given in equations 10 and 11 the following relationship can be found

$$\bar{Q}_1 = Q_1^\circ + Q^e + (n_1 + n_2)(dQ^e/dn_1)_{n_2,T,P}. \quad (17)$$

Since

$$(dQ^e/dn_1)_{n_2} = (dQ^e/dx_1)_{n_2}(dx_1/dn_1)_{n_2} \quad (18)$$

and

$$dx_1/dn_1 = x_2/(n_1 + n_2) \quad (19)$$

the equation

$$\bar{Q}_1 - Q_1^\circ = Q^e + x_2 dQ^e/dx_1 \quad (20)$$

can be written. Therefore, the derivative of the excess quantity with respect to x_1, multiplied by x_2, plus the

excess quantity for each Redlich-Kister term yields the Redlich-Kister equation for the partial molal quantity. For example, the excess quantity for the D term is

$$Q_D^e = x_1(1 - x_1)D(2x_1 - 1)^3 \qquad (21)$$

so that

$$Q_D^e + x_2(dQ^e/dx_1) = Dx_2[(1 - 2x_1)(2x_1 - 1)^3 + 3(2x_1 - 1)^2 2(x_1 - x_1^2)] \qquad (22)$$

and

$$Q_D^e + x_2(dQ^e/dx_1) = Dx_2[(1 - 2x_1)(2x_1 - 1)^3 + 6(2x_1 - 1)^2(x_1 - x_1^2)] + D[(x_1 - x_1^2)(2x_1 - 1)^3] \qquad (23)$$

This simplifies to

$$Q_D^e + x_2(dQ^e/dx_1) = D(2x_1 - 1)^2[3x_1^2 - 2x_1^3 - x_1 + 10x_1x_2 - 10x_1^2x_2 - x_2] \qquad (24)$$

Then using the relation $x_1 + x_2 = 1$, the equation can be rearranged to give

$$Q_D^e + x_2(dQ^e/dx_1) = x_2^2D(8x_1 - 1)(2x_1 - 1)^2. \qquad (25)$$

The Two Component Phase Diagram

To calculate a two component phase diagram one must be able to calculate the activity at any composition over the temperature range of interest. Redlich-Kister coefficients for the logarithm of the activity coefficient, $\log\gamma$, can provide information about the activity's dependence on composition through the equation

$$a = \gamma x \tag{26}$$

where a is the activity and γ is the activity coefficient. At other temperatures the logarithm of the activity coefficient can be calculated from the equation

$$d\log\gamma/d(1/T) = (\overline{H}_1 - H_1^\circ)/19.14464. \tag{27}$$

This equation is derived from the Gibbs-Helmholtz relationship. Therefore, if accurate enthalpy and heat capacity data as a function of temperature and composition are available, the Redlich-Kister coefficients for $\log\gamma$ can easily be calculated.

The phase diagram lines represent the point at which different species are in equilibrium. Therefore, if thermodynamic data are available for each of the species involved in a particular equilibrium, the equilibrium constant can be calculated for that reaction. The equilibrium constant can also be calculated from the activities of each species involved in the equilibria raised to the appropriate stochiometric power. Thus, the mole fraction at which equilibrium exists can be calculated for a particular temperature.

For example, suppose one is calculating the equilibrium curve for the melting of a solid into two liquid species. The equation for this reaction might be

$$Y_2Z_{(s)} = 2Y_{(l)} + Z_{(l)}. \tag{28}$$

The equilibrium constant for this reaction can easily be

calculated from $\Delta H°$ at 298.15 K and the Planck function for each of the species at the temperature of interest using the following equation:

$$K_{eq} = 10^{(-\Delta H°/19.14464T)}\ 10^{(\Delta Y_T/19.14464)}. \quad (29)$$

The equilibrium constant can also be calculated from the activities of each species by the equation:

$$K_{eq} = (a_Y^2 a_Z)/(a_{Y_2Z}). \quad (30)$$

However, the activity of the solid is normally equal to one so that this equation becomes

$$K_{eq} = a_Y^2 a_Z. \quad (31)$$

Substitution of the Redlich-Kister coefficients for log into this equation, we get

$$K_{eq} = x_Y{}^2 x_Z\ 10^{(2\log \gamma_Y)}\ 10^{(\log \gamma_Z)} \quad (32)$$

which becomes

$$K_{eq} = x_Y{}^2\ 10^{2(x_Z)^2[A + B(4x_Y - 1) + \ldots]}\ x_Z\ 10^{(x_Y)^2[A + B(4x_Y - 3) + \ldots]}. \quad (33)$$

With this equation the mole fraction at which the equilibrium point lies for a particular temperature can be calculated by a minimization process. By repeating this calculation at various temperatures the equilibrium curve can eventually be drawn.

Extended Redlich-Kister Notation

In describing phase diagrams of three or more components, R. A. Howald and I. Eliezer[13,14,15]

developed an extended Redlich-Kister notation which describes the mole fraction term for a particular coefficient. The coefficients through the seventh power, F, are shown in Table 1 for a three component system.

Table 1. The Redlich-Kister coefficients for a three component system through seventh power in mole fraction.

A_{12}	A_{13}	A_{23}				
B_{12}	B_{13}	B_{23}	B^{a}_{123}			
C_{12}	C_{13}	C_{23}	C^{a}_{123}	C^{b}_{123}		
D_{12}	D_{13}	D_{23}	D^{a}_{123}	D^{b}_{123}	D^{c}_{123}	
E_{12}	E_{13}	E_{23}	E^{a}_{123}	E^{b}_{123}	E^{c}_{123}	E^{d}_{123}

The first three columns in Table 1 represent the binary terms for the three binary subsystems present in the ternary. For the excess quantities the mole fraction terms multiplied by the Redlich-Kister coefficient are $A_{12}x_1x_2$, $E_{13}x_1x_3(x_1 - x_3)^4$, $F_{23}x_2x_3(x_2 - x_3)^5$, etc. The coefficients left over are the three component terms. The number of superscripts on these terms is always two less than the number of subscripts. The minumum number of subscripts allowed for a letter is two. This can only occur with binary terms. The maximum allowable number of

subscripts is equal to one more than the letter's position in the alphabet. However, the actual number of subscripts is equal to the number of components in the system. For example, the maximum number of subscripts for E is six; however, in a ternary system this is limited to three subscripts.

Table 2 is useful in correlating coefficients and superscripts with their appropriate powers. The first mole fraction terms are indicated by the subscripts. For example E^{b}_{123} is a sixth power term in mole fraction. This is because E is the fifth letter in the alphabet. In all cases one gets the power by adding one to the number representing position in the alphabet. The first three mole fraction terms are $x_1x_2x_3$ corresponding to each of the subscripts. The next mole fraction term is calculated from $(V - x_i)^m$ where m is equal to the number of the capital letter which is six for E, minus the number of subscripts, minus the number for each superscript. Thus in this case $m = 6 - 3 - 1 = 2$. V is the sum of each of the first mole fraction terms in this case $V = x_1 + x_2 + x_3$, and i is the first subscript. There is also a term Z^n associated with each superscript; n is the corresponding number associated with the superscript in the above scheme. Z is defined as $(x_j - x_k)$, where j is the second subscript from the left and k is the subscript correlated

with the superscript. The superscript is correlated with the subscript of the Redlich-Kister coefficient from the right. For example, the term E^{ca}_{1234} has (a) correlated with 4 and (c) is correlated with 3. Thus for E^{b}_{123} the complete term is

$$E^{b}_{123}x_1x_2x_3(V - x_1)^2(x_2 - x_3)^1$$

which is

$$E^{b}_{123}x_1x_2x_3(x_2 + x_3)^2(x_2 - x_3)^1$$

This notation can also be used for higher component diagrams. For example:

$$E^{bb}_{1234}x_1x_2x_3x_4(x_2 - x_4)(x_2 - x_3)$$

$$C^{b}_{641}x_6x_4x_1(x_4 - x_1)$$

and

$$D^{ba}_{3254}x_3x_2x_5x_4(x_2 - x_5).$$

Table 2. Redlich-Kister coefficients and their subscripts correlated with their corresponding powers

		A	B	C	D	E	F	G	H
0	1	2	3	4	5	6	7	8	9
a	b	c	d	e	f	g	h	i	j

The Higher Component Systems

For a three component system that includes mole fraction terms up to the seventh power, that is F, there must be at least fifteen terms present. There are also twenty of the four component terms for the excess

quantity. These terms are presented in Table 3, in the order that they are entered into the computer program.

However, the excess quantity is not enough. Expressions for the partial molal quantities are also needed. This can be accomplished as in the two component case by taking the derivative of the excess terms with respect to n, the number of moles.

Table 3. The three and four component Redlich-Kister coefficients

THE THREE COMPONENT TERMS

B^{a}_{123}	C^{a}_{123}	C^{b}_{123}	D^{a}_{123}	D^{b}_{123}	D^{c}_{123}
E^{a}_{123}	E^{b}_{123}	E^{c}_{123}	E^{d}_{123}	F^{a}_{123}	F^{b}_{123}
F^{c}_{123}	F^{d}_{123}	F^{e}_{123}			

THE FOUR COMPONENT TERMS

C^{aa}_{1234}	D^{aa}_{1234}	D^{ab}_{1234}	D^{ba}_{1234}	E^{aa}_{1234}	E^{ab}_{1234}
E^{ba}_{1234}	E^{ac}_{1234}	E^{bb}_{1234}	E^{ca}_{1234}	F^{aa}_{1234}	F^{ab}_{1234}
F^{ba}_{1234}	F^{ac}_{1234}	F^{bb}_{1234}	F^{ca}_{1234}	F^{ad}_{1234}	F^{bc}_{1234}
F^{cb}_{1234}	F^{da}_{1234}				

THE ONE COMPONENT PHASES

Equations of State for Magnesium Oxide

The volume as a function of temperature of MgO is well known at temperatures up to 1700 K, and the volumes tabulated by Touloukian[16] are easily fit by a quartic in (T - 1000 K):

$$V = 11.5643\,[1 + .434332 \times 10^{-4}(T - 1000) + 567479 \times 10^{-8}\,(T - 1000)^2 - .502119 \times 10^{-12}\,(T - 1000)^3 + .821952 \times 10\text{-}15\,(T - 1000)^4]. \quad (34)$$

Figure 1 shows values of the thermal expansion coefficient, α, calculated from this polynomial, the tabulated volumes by Touloukian,[10] and the volume polynomial from Howald, Moe and Roy.[25] It is clear that the volume dependence upon temperature from Howald, et al.[25] has been given excess curvature by the least squares procedure. The straight line between 300 and 1700 K is given by the equation

$$\alpha = 0.0000435 + 1.0 \times 10^{-8}\,(T - 1000). \quad (35)$$

The volumes from the thermal expansion equation and the volume polynomial in temperature agree within ± .001 cm^3/mole. The low temperature data [17,18,19,20] cited by

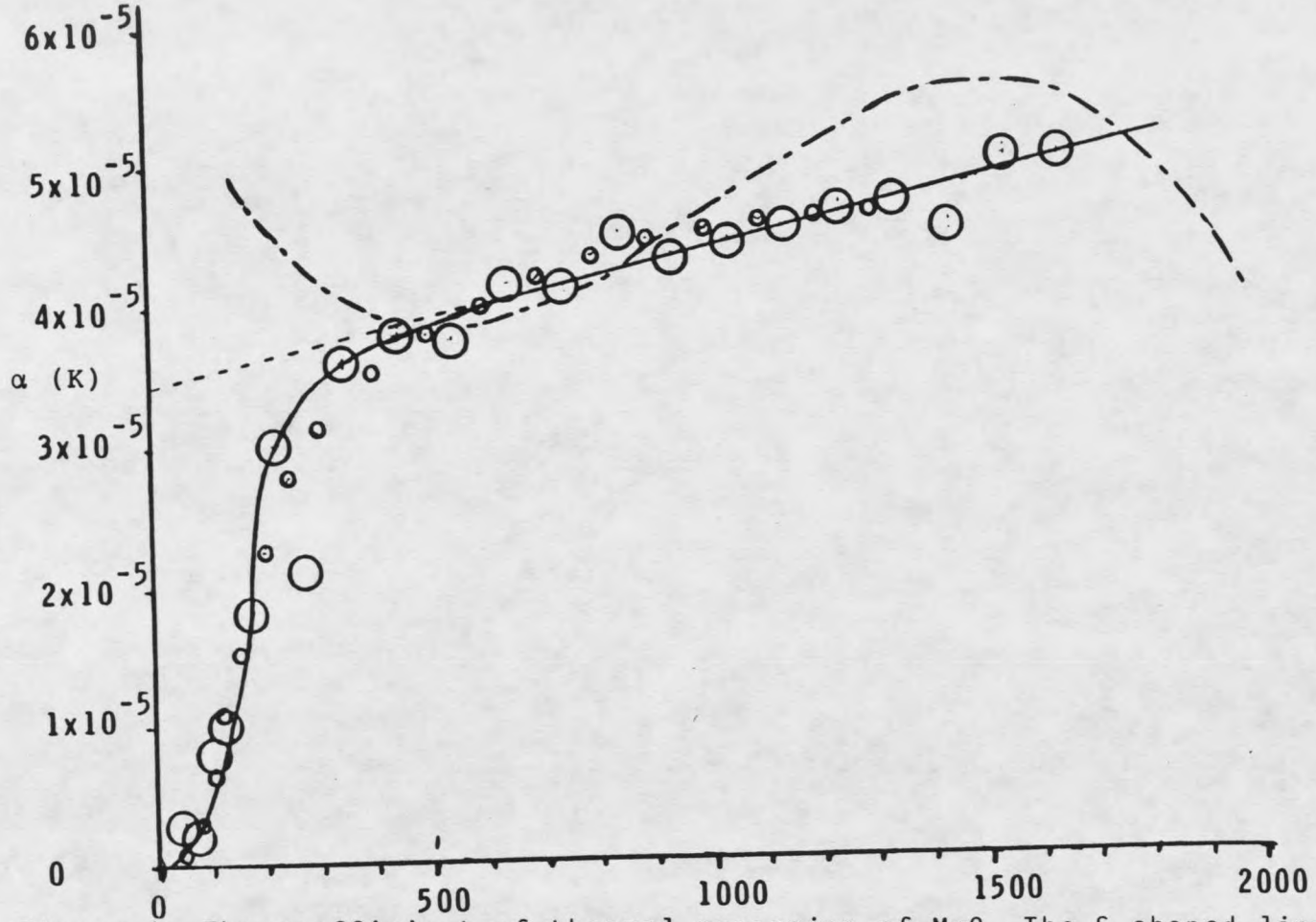

Figure 1. The coefficient of thermal expansion of MgO. The S shaped line with alternating long and short dashes represents the values used in ref.25. The straight dashed line is $.0000435+1.0\times10^{-8}(T-1000)$. The solid line shows the values selected in this work . Above 300K the solid line is that calculated from ref.16,17, and 20.

Touloukian[16] extends down to 4 K so that it is possible to sketch a reasonable curve between 400 and 0 K. The solid line in this region of Figure 1 gives volumes at 0 and 100 K of 11.1996 and 11.2016 cm^3/mole respectively.

However, it is also extremely important to have accurate data on the compressibility of MgO as a function of temperature and pressure. The Murnaghan logarithmic equation of state[21,22] has been widely used[22,23,24,25] to express the pressure dependence of the bulk modulus (K). The equation is

$$K = K_o + NP \tag{36}$$

where K_o is the bulk modulus at a standard pressure, N is a constant and P is the pressure. This equation is accurate and is easily extrapolated to high pressures, so that with a few measurements of K at various pressures a value for N can be determined.

There have been various expressions for the temperature dependence of the bulk modulus. Equations such as

$$K_{oT} = K_{oo} - CT \tag{37}$$

where, K_{oo} is the bulk modulus at a standard temperature and pressure, have been used empirically[24,25] and derived theoretically;[26,27,28] however, they are probably too simple. For example, the values for dK/dT obtained for MgO by Spetzler[24] are 27.2 to 30.1 MPa/K. These values

are inconsistent with the value calculated from Swalin's equation[26]

$$dK_S/dT = 2\gamma^2 C_p/V = 20.7 \text{ MPa/K} \quad (38)$$

where K_S is the adiabatic bulk modulus and is the Gruneisen parameter. The Gruneisen parameter is

$$\gamma = \alpha V/K_T C_V. \quad (39)$$

The difference between the adiabatic bulk modulus, K_S, and the isothermal bulk modulus K_T cannot account for this discrepancy.

Howald, Moe and Roy[25] have used the Murnaghan logarithmic equation of state

$$V = V_o(1 + NP/K_o)^{-1/N}, \quad (40)$$

but a constant value of N results in negative coefficients of thermal expansion at high temperatures and pressures. They solved this problem by including a temperature dependence for N for MgO, $AlO_{1.5}$ and $MgAl_2O_4$. However, the temperature dependence of N in the exponent greatly complicates obtaining derivatives. Also, increasing K to a value large enough to avoid negative values is inconsistent with Spetzler's[24] measurements. Also, using a positive value for dN/dT is not satisfactory, as the following derivation shows. The equation

$$d\alpha/dP = (dK/dT)/K^2 \quad (41)$$

can be easily derived from

$$d^2V/dTdP = d^2V/dPdT \quad (42)$$

and the definitions of α and K,

$$\alpha = (1/V)(dV/dT)_P \tag{43}$$

and

$$K = 1/\beta = -V(dP/dV)_T. \tag{44}$$

If the Murnaghan logarithmic equation of state is used, the expression for the pressure dependence of the coefficient of thermal expansion becomes by substitution,

$$d\alpha/dP = [(dK_o/dT) + P(dN/dT)]/(K_o + NP)^2. \tag{45}$$

The term dK_o/dT is negative and at low pressures is dominant, so that $d\alpha/dP$ is negative at low pressures as is expected. If dN/dT is positive then at higher pressures $d\alpha/dP$ becomes less negative, as it should be. However, with dN/dT being positive, there is some finite pressure at which $d\alpha/dP$ becomes positive. This can not happen, because as P approaches infinity the volume and the coefficient of thermal expansion must approach zero. This can be derived assuming that the nearest neighbor forces for any interatomic potential do not become infinite at a separation greater than zero.

It is entirely possible that the Murnaghan logarithmic equation of state is only valid over a finite temperature range. However, any correct high pressure equation of state must give volumes equal to zero as P approaches infinity, and must represent a mathematical form for the repulsive terms of the interatomic

potentials. Therefore any high pressure equation of state should be somewhat consistent with the Murnaghan logarithmic equation of state. Thus, we were led to consider the Murnaghan logarithmic equation of state as being valid to high pressures.

Spetzler's experimental measurements[24] indicate that dN/dT is zero. If this is correct then the pressure dependence of the thermal expansion coefficient becomes,

$$d\alpha/dP = (dK_o/dT)/(K_o + NP)^2. \tag{46}$$

This can be integrated to give

$$\alpha = -(dK_o/dT)/N(K_o + NP). \tag{47}$$

Thus, both α and β approach zero linearly in $1/(K + NP)$ as the pressure approaches infinity.

Rearranging and integrating this equation for α, we obtain

$$K_{oT} = K_{oT_o} \exp(-N \int_{T_o}^{T} \alpha dT) = K_{oT_o}(V_{T_o}/VT)^N \tag{48}$$

where T_o is a standard temperature at which the low pressure bulk modulus is K_{oT_o}.

While there are usually sufficient data to evaluate V and α at high temperatues, there is very little data for the evaluation of the bulk modulus at these high temperatures. Therefore, if this equation is at all correct, it will be extremely useful.

There is good agreement[24,17,18,19,20] on the value of K_o = 160100 MPa for MgO at 298.15 K. We first used

Spetzler's[24] value of N = 3.9; however, this gives values of dK_o/dT of about -15 MPa/K. This is definitely not steep enough to match either Spetzler's[24] or Soga and Anderson's[29] data. Anderson's 1968 review[30] gives N = 4.50 and 4.58 for single crystal and polycrystalline MgO respectively. We finally chose a value of N = 4.57 for our calculations, which is taken from Carter, et al.,[31] and is consistent with other measurements.

With values of N and $K_{o,298.15}$ chosen, we can calculate K_o at any temperature from the relationship

$$K_{oT} = K_{oT_o}(V_{T_o}/V_T)^N. \tag{49}$$

Most experimental methods give the adiabatic bulk modulus instead of the isothermal bulk modulus, but this can easily be corrected through the equation

$$K_s = K/(1 - \alpha^2 VKT/C_p). \tag{50}$$

This equation gives K_s = 163062 and 150082 MPa at 300 and 1000 K respectively. For temperatures below 300 K, values for α were determined from the curve shown in Figure 1, and C_p values were taken from the JANAF tables[32] and the Barron paper[33] to get $K = K_s$ = 163137 MPa at 0 K. The full set of calculated K_s values is plotted in Figure 2. The calculated curve is in excellent agreement with the 300 and 800 K values of Spetzler[24] and the 296 value of Anderson and Andreatch.[34] Anderson and Andreatch's value[34] at 77 K and all the values of Soga and Anderson[29]

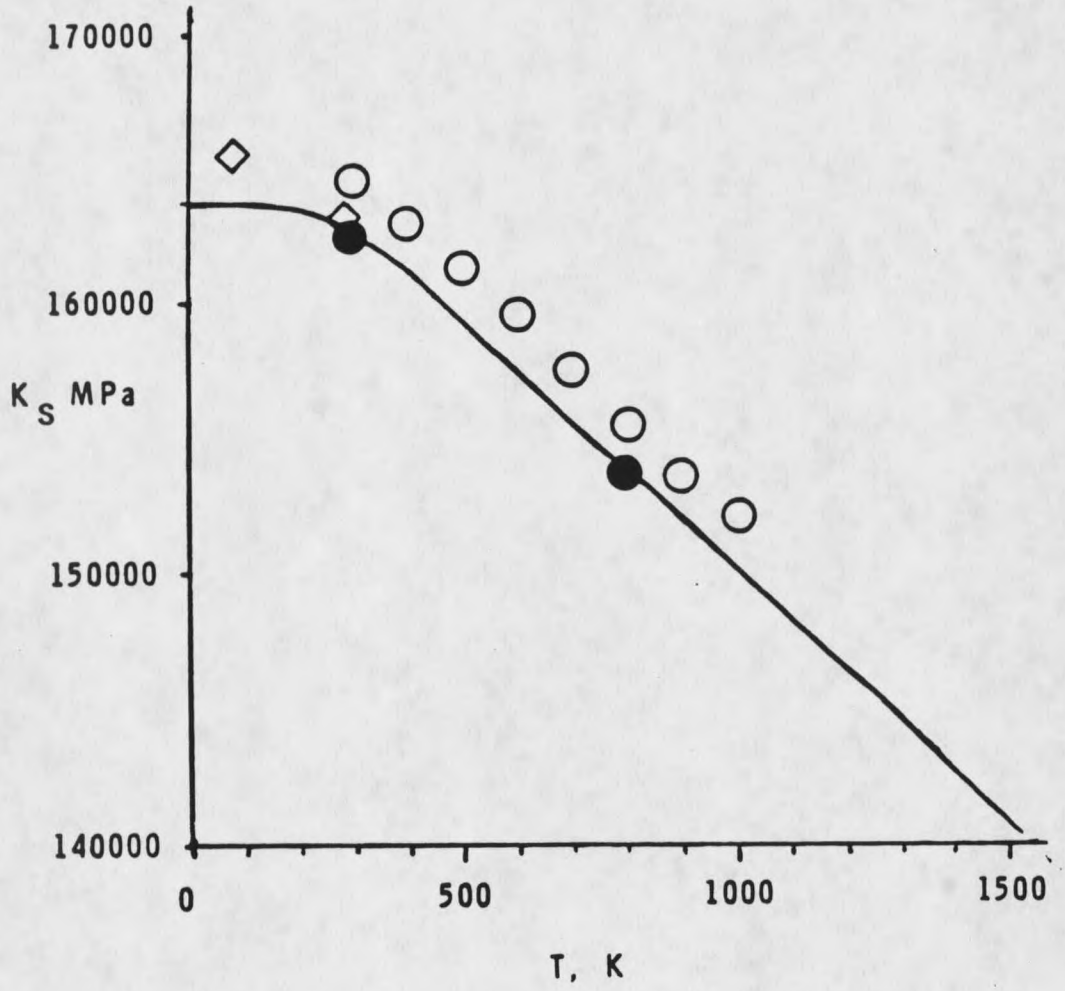

Figure 2. The isoentropic bulk modulus for MgO. The solid line is calculated from the theory presented here. The experimental values are from Spetzler, black circles; Soga and Anderson, open circles; and from Anderson and Andreatch, diamonds.

are about 1% higher that the calculated curve, but this is within the experimental error. Therefore, the data for MgO are in full agreement with the predictions assuming the validity of the Murnaghan logarithmic equation of state to high pressures with a constant value of N = 4.57.

Table 4 provides calculated molar volumes at various pressures for MgO for comparison with the calculated volumes of Howald, et al.[25] The values at 0.1 and 900 MPa agree with Howald, et al.[25] within ± 0.01 cm^3/mole. At 30,000 MPa our values are 0.05 to 0.06 cm^3/mole larger. This is due to the larger value of N that we are using.

Table 4. Calculated molar volumes for MgO

	P,MPa			
T,K	.01	9000	15000	30000
300	11.2464	10.6974	10.4025	9.8223
650	11.3956	10.8094	10.4980	9.8912
1000	11.5643	10.9341	10.6035	9.9665

Once these calculations using the Murnaghan logarithmic equation of state are done it is a simple matter to calculate the volume polynomial's dependence on pressure. The completed volume polynomials for MgO(c) and MgO(l) are given in Table 5, along with the heat capacity

Table 5. The equations of state, heat capacity equations and selected thermodynamic properties of MgO (c) and MgO (l)

MgO (S) VOLUME POLYNOMIAL

11.56431	4.3773181E-5	5.6747946E-9	-5.02119E-13	8.219519E-16
-7.096668E-6	-1.728388E-9	-3.96682E-13	-4.12045E-17	-3.69883E-20
1.402579E-10	6.210500E-14	2.043779E-17	4.563120E-21	2.019368E-24
-3.36068E-15	-2.15203E-18	-9.20887E-22	-2.99147E-25	-1.16580E-28
8.593206E-20	7.114327E-23	3.704788E-26	1.538755E-29	6.128646E-33
-2.00574E-24	-1.96492E-27	-1.16729E-30	-5.66303E-34	-2.35995E-37
2.819661E-29	3.033287E-32	1.941636E-35	1.027253E-38	4.424865E-42

MgO (LIQUID) VOLUME POLYNOMIAL

13.993	.437732E-04	.567479E-08	-.502119E-12	.821952E-15
-.709667E-05	-.172839E-08	-.396682E-12	-.412045E-16	-.369883E-19
.140258E-09	.621050E-13	.204378E-16	.456312E-20	.201937E-23
-.336068E-14	-.215203E-17	-.920887E-21	-.299147E-24	-.116580E-27
.859321E-19	.711433E-22	.370479E-25	.153875E-28	.612865E-32
-.200574E-23	-.196492E-26	-.116729E-29	-.566303E-33	-.235995E-36
.281966E-28	.303329E-31	.194164E-34	.102725E-37	.000000E+00

HEAT CAPACITY C_p

	A[a]	B	C	D	E
MgO (S)	51.0941	.00310468	-5.56218E-07	2.747330E-10	-1.26513E+06
MgO (L)	53.6488	.0032598	-5.84029E-07	2.884697E-10	-1.32839E+06

THERMODYNAMIC PROPERTIES	Y_{1000} J MOL^{-1}	$H_{1000}-H_{298}$ J MOL^{-1}	H_{298} J MOL^{-1}	S_{298} J MOL^{-1} K^{-1}	V_{1000} CM^3
MgO (S)	49.27	3.2974E+4	-6.01490E+5	26.94	11.248
MgO (L)	63.10923	34623.	-551278.3	35.	11.81

[a] THE HEAT CAPACITY EQUATIONS ARE GIVEN BY $Cp = A + B \times 10^{-2}(T-1000) + C \times 10^{-6}(T-1000) + D \times 10^{-9}(T-1000) + E \times 10^{7}(T^{-2}-10^{-6})$

equations and selected thermodynamic values. The heat capacity equation for MgO(c) and the ΔH_{fus} are taken from Howald, et al.[25] The ΔH_{fus} is 57.65 KJ/mole. Thus the solid is fully described and can be used to calculate equilibrium constants for any reaction in which it is involved.

For MgO liquid there are few measurements of volume or heat capacity. From the volume and heat capacity changes in the fusion of the alkali halides we have estimated the volume and the heat capacity of the liquid to be 21% and 5% greater than that of the solid.

In order to compare the equations of state considered here with other proposed equations, we have calculated Gruneisen,

$$\gamma = KV/C_V, \tag{51}$$

and the Anderson-Gruneisen,

$$\delta = (dK_S/dP)_T - 1, \tag{52}$$

parameters for MgO over a wide range of temperatures and pressures. These parameters show a small but not negligible dependence upon both the pressure and temperature. The results of γ are shown as contour lines in Figure 3. Figure 4 shows that the values of the Gruneisen parameter for MgO calculated from our equation of state are approximately consistent with the commonly assumed form

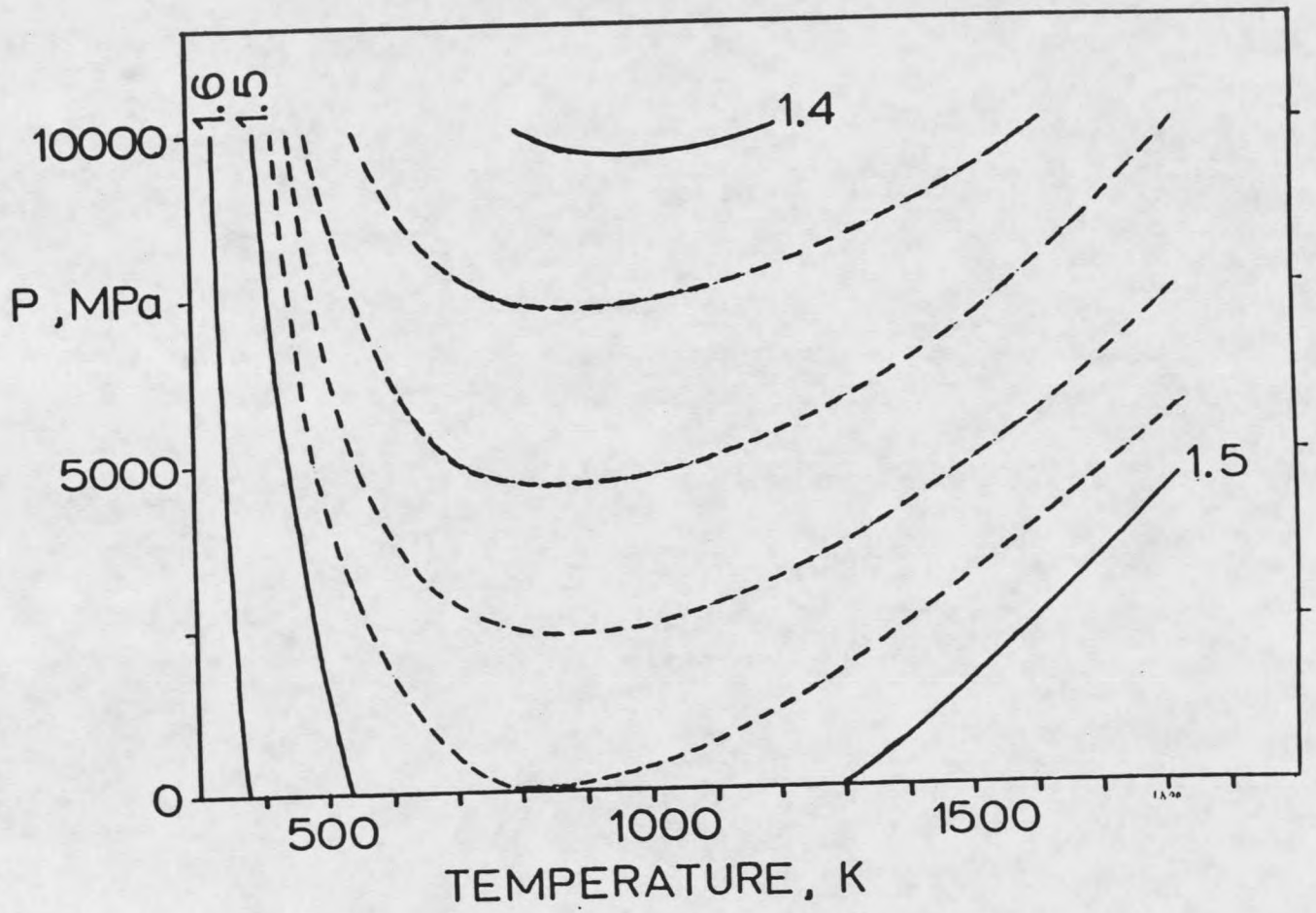

Figure 3. Contour lines for the Gruniesn parameter, γ, for MgO on a P-T field. The contour interval is 0.01, except that at high temperatures dotted lines at 0.02 intervals are also shown.